Modification of curing, morphological, mechanical and electrical properties of epoxidised natural rubber (ENR-25) through the addition of copper calcium titanium oxide (CCTO)

Syifa' Muhammad Sharifuddin[1] · Mohd Shukri Mat Nor[1] ·
Fathin Asila Mohd Pabli[1] · Wannarat Chueangchayaphan[2] ·
Zainal Arifin Ahmad[3] · Muhammad Azwadi Sulaiman[1]

Abstract

The limited applicability of very high dielectric permittivity ceramic materials such as copper calcium titanium oxide, commonly known as CCTO ($\varepsilon_r = 100,000$ at room temperature and nearly independent of frequency from 1 Hz to 1 MHz), could be improved through the fabrication of polymer matrix composites. Ceramic is brittle while polymers are materials that are ductile and have excellent flexibility but low ε_r. Another contrast between the two materials is the fabrication process where ceramic, specifically, requires pressing and a high sintering temperature. Hence, the right combination of ceramic and polymeric materials should theoretically produce a composite with excellent mechanical and electrical properties. Therefore, a study on CCTO ceramic powder blended with 25 mol% of epoxidised natural rubber (ENR-25) was carried out. The CCTO powder was initially synthesised through solid-state reaction followed by compounding with ENR-25 formulations with different CCTO loadings (0, 20, 40, 60, 80, 100, and 120 phr) in an internal mixer. Small blocks of the composite were cast into ~2 mm of mould thickness and then hot compressed into square shapes. Samples were characterised by curing, mechanical, electrical, and microstructural properties. As a result, the addition of CCTO was found to have lowered the curing time, i.e. tc_{90} at 20 phr, compared to composites without CCTO loading. Then, the curing time gradually increased with filler loading from 2.05 to 2.48 at 20 to 120 phr loading, respectively. Mechanical testing of the composites showed an increase in tensile strength from 5.91 to 16.46 MPa. However, with content higher than 40 phr content, the tensile strength's magnitude gradually decreased with increasing filler loading from 13.63 to 6.49 MPa. In comparison, hardness properties increased with an increase of filler loading from 30.5 to 44.7 Shore A. Meanwhile, LCR meter showed that increased CCTO content could improve ε_r value from 6.134 to 12.114 at 75 kHz and decrease the dielectric loss

Extended author information available on the last page of the article

▲ Springer

(tan δ) from 0.179 to 0.150 at 2 MHz. The composite's microstructure also shows CCTO crystals embedded in the ENR-25 with excellent surface contact. The surface morphology showed that samples with filler content of 60 phr onwards had a lot of CCTO particle pore agglomeration, which reduced its mechanical strength from 16.46 to 6.49 MPa.

Keywords Properties modification · Dielectric properties · Mechanical properties · CCTO/ENR-25 composite

Introduction

Recent years have witnessed a growing academic interest in polymer-ceramic composites. A flexible material with high ε_r and excellent mechanical properties can be used in a wide variety of electromechanical applications such as for energy storage, capacitors, antenna, electronic packaging, and actuators [1–4]. The combination of the desired characteristics of high dielectric materials with improved mechanical properties leads to the fabrication of polymer/ceramic composites. Ceramic materials have always been known for their high ε_r and relatively low dielectric loss (tan δ) [5]. However, its main drawbacks are its brittleness as well as its high sintering temperature which leads to the requirement for high processing temperatures of more than 1000 ℃ [6]. In contrast, polymers have low dielectric properties but excellent mechanical properties and require low processing temperatures. The current demand for the incorporation of artificial intelligence (AI) technology drives new research on a next-generation dielectric material. These new dielectric materials should possess high ε_r, low tan δ, low processing temperature, easy fabrication, low cost, and most importantly, the ability to satisfy the market's needs.

Material selection plays a vital role in determining and designing a new application. Therefore, calcium copper titanate ($CaCu_3Ti_4O_{12}$: CCTO) was selected due to its high dielectric properties. CCTO was first synthesised in 1967 by Alfred Deschanvres and his co-workers without knowing its enormous benefit. After three decades, the discovery of dielectric properties of CCTO by Subramanian et al. [7] triggered a vast amount of innovative scientific inquiry. ε_r value for CCTO can reach up to 100,000 at room temperature and is low-temperature dependent [8] which are essential traits required in electronic devices and systems. The study [7] shows that oxides with a perovskite structure will exhibit high ε_r, but unfortunately, most are ferroelectric or temperature-dependent. However, CCTO is not a temperature-dependent property material; therefore, many researchers have shifted their interest to CCTO [9]. Much research has been reported on polymer composites using high ε_r materials such as barium titanate ($BaTiO_3$) and lead zirconate (PZT) [6, 10]. Unfortunately, both materials have weaknesses; for example $BaTiO_3$ is a temperature-dependent dielectric material while PZT is harmful to health.

Natural rubber (NR) is a polymer under the elastomer group and is derived from the latex of the *Hevea brasiliensis* tree. NR has attractive physical and chemical properties comparable to synthetic rubber [11]. It is favoured due to its low-temperature

flexibility, high elasticity, fatigue resistance, environmental friendliness, and tear-resistance [12]. However, NR is a weak polar group [13] which caused researcher interest to shift to ENR or epoxyprene. ENR is the product of the epoxidisation of NR using peracetic acid. The reaction from peracid leads to isoprene backbone modification which also improves its properties, as shown in studies of gelling [14] and its polarity [15]. Composites consist of two or more distinct physical and chemical properties that can differ by reinforcement and matrix. Surprisingly, the CCTO/ENR-25 composite has still not been systematically studied. Therefore in this study, CCTO was chosen as the reinforcement and 25% mol of epoxidised natural rubber (ENR-25) as the matrix. This study aimed to determine the mechanical, electrical, and microstructural properties of the CCTO/ ENR-25 composite.

Experimental procedure

Materials

Analytical reagent grade calcium carbonate ($CaCO_3$), copper (II) oxide (CuO), and titanium dioxide (TiO_2) were obtained from R&M Chemicals (Malaysia) and used to synthesise CCTO. Methanol (JT Baker, Malaysia) was used as a grinding medium. Zirconia balls, polyurethane mill jar, and milling machine were supplied by Magna Value, Malaysia. The starting materials used for the fabrication of CCTO/ ENR-25 composites were epoxidised natural rubber with 25% mol epoxide (ENR-25), zinc oxide (ZnO), stearic acid (activators), Mercaptobenzothiazole (MBT) (accelerator), and sulphur (curing agent): ENR-25 was supplied by Muang Mai Guthrie Public Co., Ltd. (Surat Thani, Thailand), ZnO and stearic acid were purchased from Bossoftical Public Co., Ltd. (Songkhla, Thailand) and MBT and sulphur were obtained from Vessel Chemical Public Co., Ltd. (Bangkok, Thailand).

Synthesis of $CaCu_3Ti_4O_{12}$ (CCTO)

CCTO was synthesised using solid-state reaction at a calcination temperature of 900 °C for 12 h using $CaCO_3$, CuO, and TiO_2 as raw materials. The same method from previous studies was adopted [8, 16]. The raw materials were firstly weighed using stoichiometric ratio and then mixed in a polyurethane mill jar for 24 h using zirconia balls as mixing media with a mass ratio of balls to raw materials of 10:1. The wet mixing technique was applied to speed up the mixing process using methanol as a mixing medium. The synthesised CCTO powder was characterised for phase formation using X-ray diffractometer (XRD Bruker D2 Phaser), particle size distribution measurement (Malvern Mastersizer MS 3000)), and particle morphology using scanning electron microscope (JOEL JSM-IT100).

Table 1 Compounding formulation of CCTO/ENR-25 composites (in phr)[a]

Ingredient	Formulation (phr)						
	0	20	40	60	80	100	120
ENR-25	100	100	100	100	100	100	100
Zinc oxide	5	5	5	5	5	5	5
Stearic acid	2	2	2	2	2	2	2
MBT	1.5	1.5	1.5	1.5	1.5	1.5	1.5
Sulphur	1.5	1.5	1.5	1.5	1.5	1.5	1.5
CCTO	0	20	40	60	80	100	120

[a]phr = part per hundreds of rubber per weight

Table 2 Mixing schedule used to prepare CCTO/ENR-25 composites

Mixing procedure	Cumulative time (min)
Step 1 Internal mixer (Brabender)	
ENR-25 mastication	0
Addition of ZnO and stearic acid	5
Addition of CCTO filler	8
Addition of MBT	11
Addition of sulphur	13
Dumping	15
Step 2 Two-roll mill	
Sandwich technique	1
Roll technique	2

Fabrication of CCTO/ENR-25 composites

CCTO/ENR-25 composites were prepared by the mixing process at 60 °C using an internal mixer (Brabender GmbH & Co, Germany) with 60 rpm rotor speed and capacity size of 70 cm^3. The composites were prepared with various CCTO loadings of 0, 20, 40, 60, 80, 100, and 120 phr, as shown in the compounding formulation in Table 1. Meanwhile, Table 2 shows the mixing schedule of composites. The ENR-25 was first masticated for 5 min and then mixed with zinc oxide and stearic acid for 3 min. The CCTO filler was added into the compound for 3 min and was continued with the addition of sulphur and MBT for 3 min, respectively. The compound was sheeted out using a two-roll mill to improve the dispersion of the added chemicals and then left at room temperature before the vulcanisation process took place using compression moulding. The rubber compound was cured and pressed into a $150 \times 160 \times 2$ mm^3 sheet mould at 160 °C for the respective cure times t_{c90} from the MDR test.

Characterisation of CCTO/ENR-25 composites

After the mixing process, a small amount (≥ 5 g) of the rubber compound was cut to analyse the cure characteristic. The cure characteristic of composites was investigated using a moving die rheometer (MDR) (model: MDRH 2020, Monsanto Co., Ltd., Ohio, USA) at 160 °C with 1° arc for 30 min. The optimum cure time (t_{c90}), scorch time (t_{s1}), minimum torque (M_L), maximum torque (M_H), delta torque (M_H–M_L), and cure rate index (CRI) were recorded. The vulcanised rubber composite sheet was cut into dumb-bell shapes using a cutting die following a standard from ASTM D-412 for characterising tensile and stress–strain behaviours of CCTO/ENR-25 composites. It was conducted using Tinius Olsen (model 10ST, Salfords, England) at 23 ± 2C with a 500 mm/min speed. Hardness properties were investigated using a standard from ASTM D2240 where 6 mm thick samples were prepared for Shore A using Durometer (Instron, Massachusetts, USA). Meanwhile, electrical properties were measured using LCR meter (NanoTec; model Agilent 4285A) at a frequency range from 75 kHz to 10 MHz. The surface morphology of the selected parts of CCTO/ENR-25 composites was observed using a scanning electron microscope (SEM)/ energy dispersive X-rays (EDX) at $500 \times$ magnification (JOEL JSM-IT100).

Results and discussion

CCTO powder characterisation

Figure 1 shows the distribution of particle size for CCTO powder produced after the calcination process. The particle size ranged from 0.571 to 29.185 μm with two normal density distributions within the range. The larger distribution is suggested to have been caused by agglomeration of smaller particles; this is indicated in particle
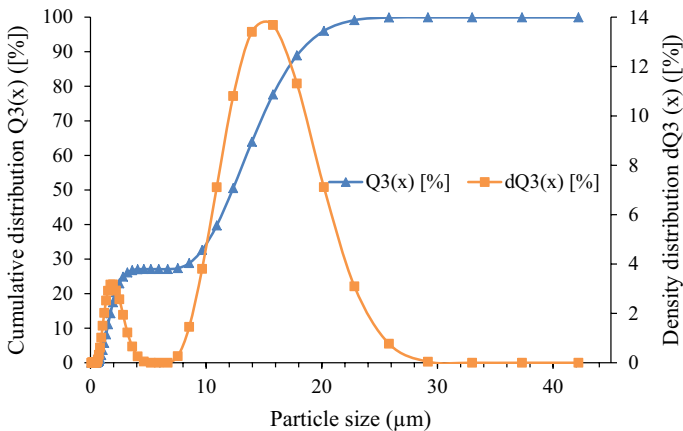

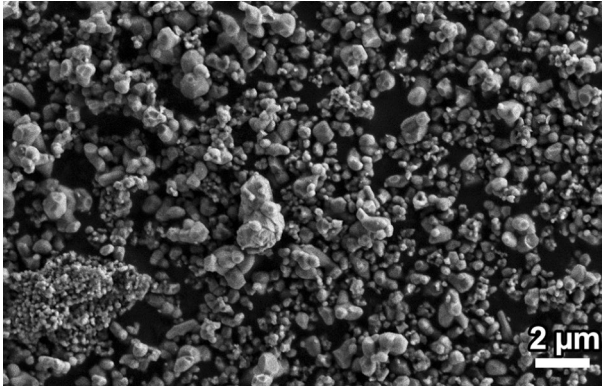**Fig. 1** Particle size distribution of the synthesised CCTO powder measured by particle sizer

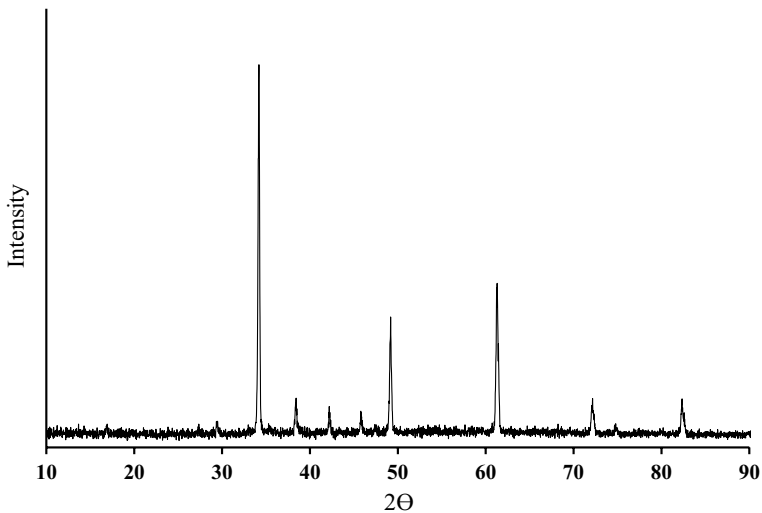**Fig. 2** Morphology of the synthesised CCTO powder observed under SEM

Fig. 3 The synthesised CCTO powder matched to ICSD 01–075-2188 ($CaCu_3Ti_4O_{12}$) X-ray diffraction pattern

morphology from SEM micrograph in Fig. 2. The particles are almost spherical in shape and some of them had already diffused to each other and grew larger. Single phase of CCTO was produced after calcination process at a temperature of 900 °C for 12 h, as shown by the XRD pattern in Fig. 3. The pattern matches the database standard of ICSD 01–075-2188 ($CaCu_3Ti_4O_{12}$).

Cure characteristics of CCTO/ENR-25 composites

The significant effects of CCTO addition on ENR-25 were studied using the MDR machine. Table 3 provides an overview of the collected data obtained from MDR

Table 3 Cure characteristic of CCTO with different filler content embedded in ENR-25

CCTO/ENR 25 content (phr)	Cure characteristic					
	t_{s1} (min)	t_{c90} (min)	M_L (dN.m)	M_H (dN.m)	M_H-M_L (dN.m)	CRI (min^{-1})
0	0.49	2.37	0.58	12.40	11.82	41.76
20	0.52	2.05	0.54	15.34	14.80	48.26
40	0.55	2.08	0.49	16.20	15.71	47.45
60	0.59	2.10	0.44	18.77	18.33	47.03
80	1.03	2.35	0.32	22.32	22.00	41.52
100	1.02	2.43	0.29	23.19	22.90	40.08
120	1.12	2.48	0.24	25.94	25.70	39.15

rheographs. The scorch time (t_{s1}) or premature vulcanisation gradually increased with CCTO addition. The increase in t_{s1} with the filler was also reported by Chuayjuljit et al. [17]. This phenomenon is due to the isolated double bond reacting more rapidly with sulphur than a continuous bond, and the epoxide group's ability to accelerate the vulcanisation process in ENR. However, the addition of CCTO lowered the epoxide group's efficiency to activate the double bonds nearby. The incorporation of CCTO filler in the composite lowered the optimum cure time (tc_{90}) at 20 phr of CCTO loading. This reduction might be due to free electrons in the CCTO and ENR network which ease the phonon transfer, resulting in increased thermal conductivity of CCTO [4, 18–20].

The tc_{90} also increased with filler loading. As reported by Luangchuang et al. [23], the phenomenon can be explained as being due to the absorption of the accelerator agent by some hydroxy groups on ceramic surfaces and higher filler loading which prevent sulphur interactions with the rubber matrix. Table 3 also presents the minimum (M_L), maximum (M_H), and delta torque (M_H–M_L). M_L, commonly addressed as elastic modulus of uncured blend [17], was shown to have decreased. Surprisingly, it is also related to the viscosity of the composite. Thus, if the viscosity of the composite is reduced, it would improve the processability of the composites [21]. M_H showed results which were the opposite of M_L. In other words, the maximum torque value represents the stiffness and hardness of the composite at the end of the vulcanisation process [17, 22, 23]. Simultaneously, delta torque (M_H–M_L) measures cross-linking behaviour, and the increasing delta torque value indicates that the cross-link density of the CCTO/ENR-25 composite increased with filler addition. This is due to a very fine CCTO powder (0.571 to 29.185 μm; Fig. 1) which directly helped the rubber processing step by behaving as a plasticiser before the vulcanisation process starts. After that, the CCTO powder behaved like an activator for vulcanisation, as can be seen with the increase in M_H-M_L value with increasing CCTO content. This observation is in-line with the tensile test, elongation at break and tensile modulus (M100 dan M300) of the samples (to be discussed in "Mechanical properties of CCTO/ENR-25 composites" Section). However, at higher amounts, CCTO powder starts to cause agglomeration (as shown in SEM micrographs; Fig. 4) which affected these values. Therefore, the incorporation of CCTO filler had improved and contributed to the cross-linking process [4, 18, 24, 25].
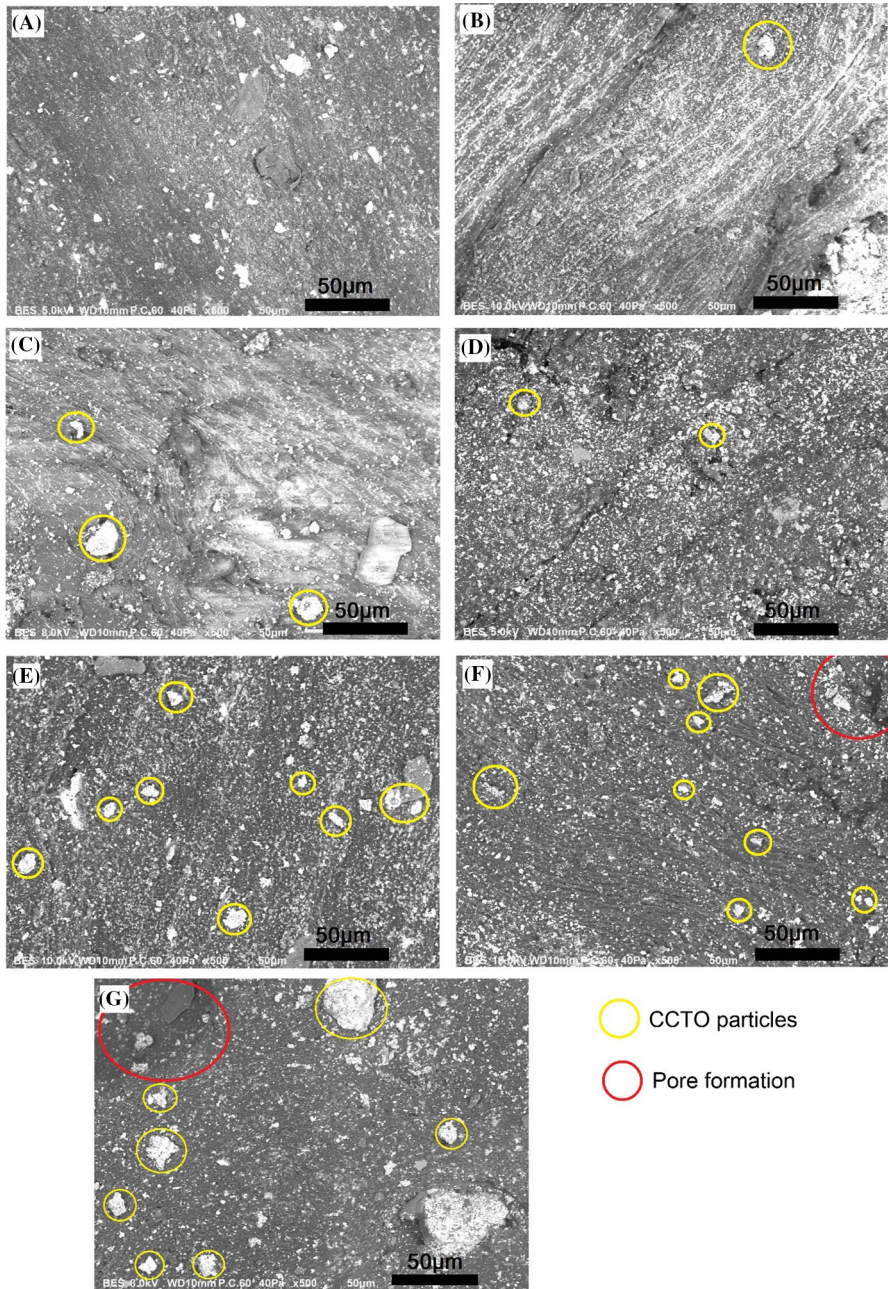
Fig. 4 Surface morphology of ENR-25/CCTO samples **a** 0 phr, **b** 20 phr, **c** 40 phr, **d** 60 phr, **e** 80 phr, **f** 100 phr, and **g** 120 phr using a scanning electron microscope at 500×magnification

Morphology characterisation of CCTO/ENR-25 composites

The dispersion of CCTO filler in the ENR-25 rubber matrix can be examined directly using SEM. The SEM micrograph of the composite surface from 0 to 120 phr is presented in Fig. 4 at 500× magnification. The powder particles present in Fig. 4(a) are the dispersion of zinc oxide, which can be clarified using EDS analysis in Fig. 5a. Figure 2 shows the EDS and element micrograph of the composites with 0 and 100 phr of filler loading. The most prominent finding to emerge from the analysis is that the size and number of agglomeration of CCTO particles (yellow circles) increased with increasing CCTO loading. As a result, the pore size also increased with CCTO loadings, leading to pore formation, as shown in Fig. 4f and g in the red circles. This is due to the electrostatic force that generates interfacial interaction between other ceramic particles like ZnO [11].

Mechanical properties of CCTO/ENR-25 composites

In addition to dielectric properties, mechanical properties also make a tremendous contribution to the design of a polymer-ceramic composite of CCTO/ENR-25. Several factors will affect the mechanical performance, such as particle morphology, size, and particle loading. Critically, filler-rubber interaction also plays an essential role in the deterioration of mechanical properties. The stress–strain
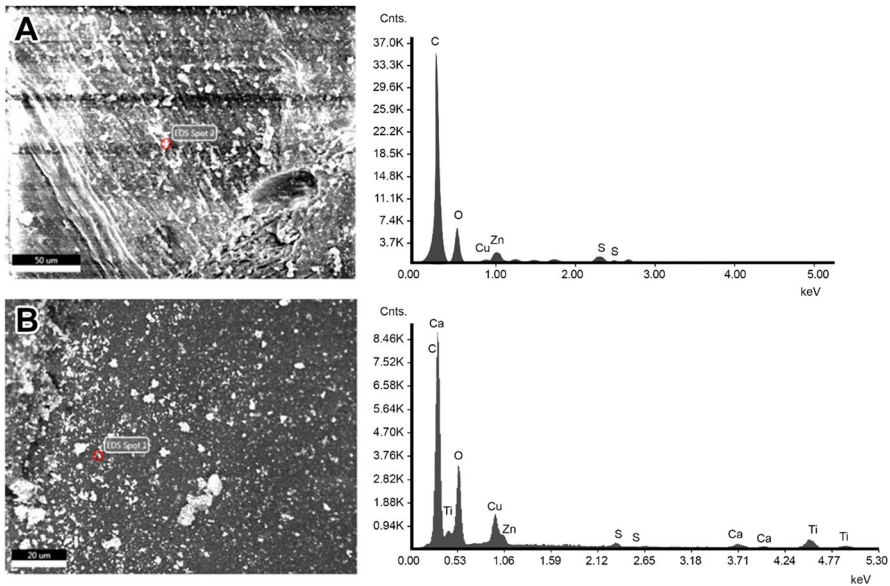

Fig. 5 Representative of EDS and element micrograph of CCTO/ENR-25 samples, **a** 0 phr, and **b** 100 phr

behaviours of the composites in Fig. 6 illustrate excellent performance along with the increasing stress–strain. However, a drastic increase was observed in all samples when strain was higher than 400% except for the compound without filler (0 phr).

Meanwhile, the CCTO/ENR-25 composite's tensile strength in Fig. 7 gradually increased with the increasing filler loading, showing a polynomial tendency of third order. The increase in tensile strength stopped at 40 phr, after which it continuously dropped. This indicates that 40 phr is the maximum filler loading with better dispersion of filler-rubber interaction. The decrease in tensile strength can be explained by the agglomeration of CCTO particles as seen in the SEM image in Fig. 4c-g, respectively. Agglomeration tends to reduce the densification of composites and increases porosity [26]. Thus, the presence of pores lowered the tensile strength of the composites. ENR-25 matrix is known as a hydrophobic material [27] while CCTO filler is hydrophilic; therefore, the combination of these materials weakened the interfacial interaction [19, 28]. Besides that, the porous structure slowly appeared in the inner structure of the CCTO/ENR-25 composite after 40 phr loading. The pore size also increased with increasing filler loading, thus inducing the stress concentration.

Elongation at break steadily decreased in linear trendline with increasing filler loading due to the high cross-link density and low filler-rubber interaction [13]. As reported by Krainoi et al. [18], the decrease of elongation at break could also happen due to the mobility of ENR being hindered by the CCTO particles. The trend for 100% modulus and 300% modulus increased with increasing filler loading, as illustrated in Fig. 8, exhibiting a polynomial tendency of the fifth order. However, at 120 phr loading for 100% modulus, it dropped. For 300%, it started
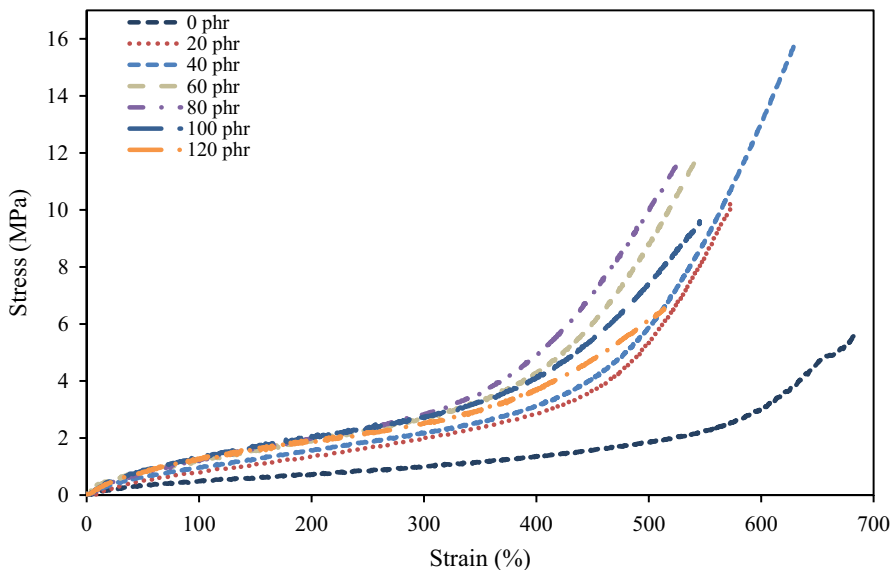

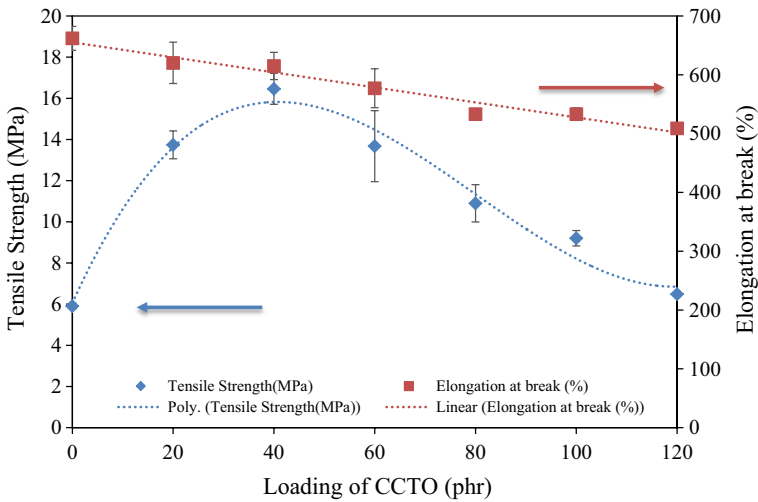**Fig. 6** Stress–strain behaviours of CCTO/ENR-25 composites at different filler loadings of CCTO

Fig. 7 Tensile strength and elongation at break of CCTO/ENR-25 composites at different filler loadings of CCTO
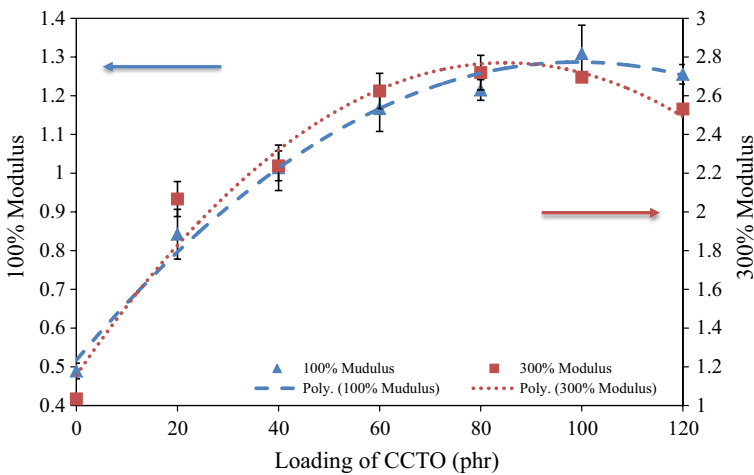

Fig. 8 100% modulus and 300% modulus of CCTO/ENR-25 composites at different filler loadings of CCTO

to drop at 100 phr loading. Therefore, the tensile strength, elongation at break, 100% modulus, 300% modulus, and hardness of the CCTO/ENR-25 were directly affected by the filler loading.

Hardness properties of the composite in Fig. 9 showed a directly proportional behaviour with a polynomial tendency from 30.5 to 44.7 Shore A. The amount of filler content does affect the rigidity and cross-link density of the rubber composite [29], resulting in resistance to the penetration of an indenter. Hardness properties of
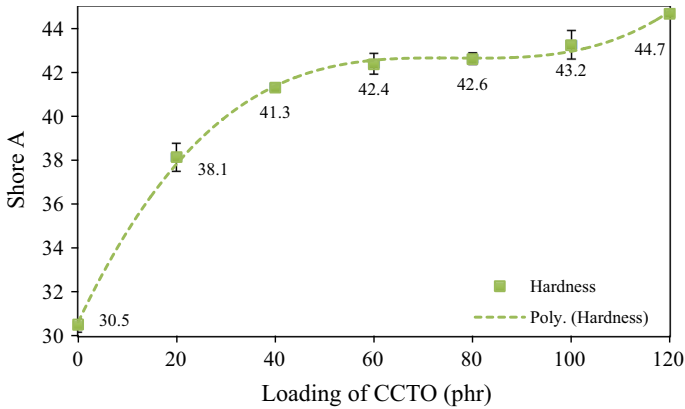
Fig. 9 Hardness properties of CCTO/ENR-25 composites at different filler loadings of CCTO

0 to 40 phr of CCTO loading sharply increases, while samples with 60 phr to 120 phr of filler loading became saturated at around 42 to 44 Shore A. This indicates that the rigidity had reached its maximum limit. The increasing hardness properties with the polynomial tendency of third order are illustrated in Fig. 9 [30].

Dielectric properties of CCTO/ENR-25 composites

Figure 10 shows an improvement in dielectric permittivity (ε_r) with increasing CCTO content from 6.13 to 12.11 at 0.1 MHz. Theoretically, the increasing filler loading will increase the dielectric properties of materials due to space charge
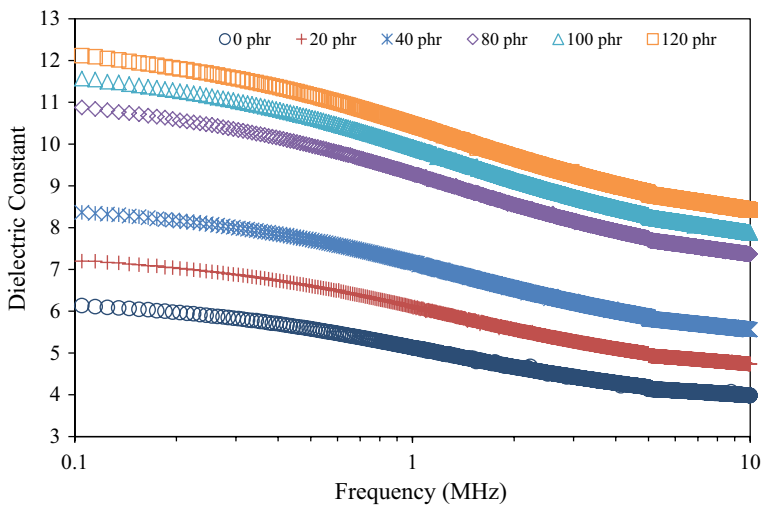

Fig. 10 Electrical properties of different filler content of CCTO embedded in ENR-25 at a different frequency range of dielectric constant

polarisation amount at the particle-rubber matrix boundary [18] and the formation of large dipoles in the ceramic particle [4]. It also shows that ε_r gradually decreases over the increasing frequency of testing. These phenomena happen due to the dielectric relaxation of ceramic particles [4] and low interfacial polarisation or the Maxwell–Wagner–Sillar effect, which exists in heterogeneous dielectric materials [18, 31, 32]. A closer inspection was done at 0.1, 1, and 10 MHz, respectively, as illustrated in Fig. 11.

Meanwhile, the dielectric loss (tan δ) of the CCTO/ENR-25 composite in Fig. 12 showed a decrease from 0.179 to 0.150 at 2 MHz of 0 phr and 120 phr, respectively. The polarisation at frequency of 0.1 to 2 MHz was common until the relaxation phenomena took place. Sulaiman et al. [8] suggested that this happens due to space charge polarisation that usually exists at low frequencies. The increase in frequency of alternating electric fields caused the polarisation left to catch up and contribute to the increase of dielectric loss. Besides that, the dielectric loss of the composite at the increased in filler loading is shown in Fig. 13. The regression analysis at frequency 0.1 and 1 MHz showed that the dielectric loss correlates with the filler content with a p-value of 0.037 and 0.001, respectively. However, at frequency 10 MHz, the p-value is 0.362, higher than 0.005 of significant value that means no statistical correlation.

Conclusion

The morphological, mechanical, and electrical properties of ENR-25 were successfully modified by adding up to 120 phr CCTO particles. However, from SEM examination, pore formation started at 60 phr onwards, significantly reducing the
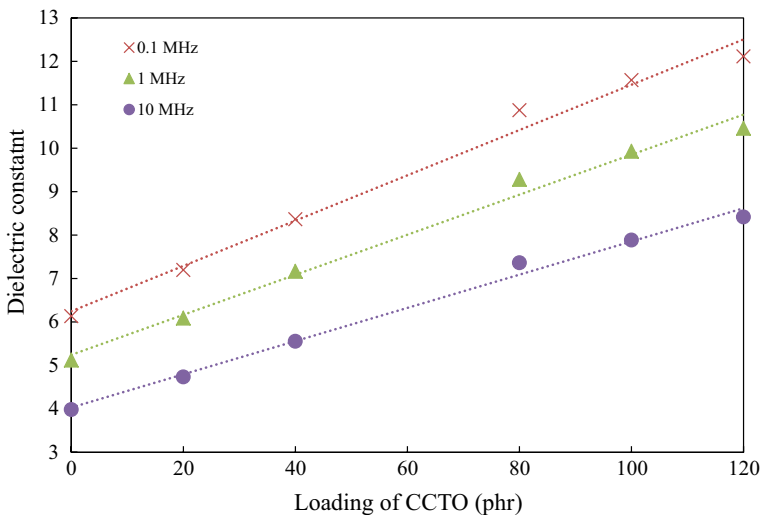

Fig. 11 Dielectric constant curve of different filler content of CCTO embedded in ENR-25 at 0.1, 1, and 10 MHz
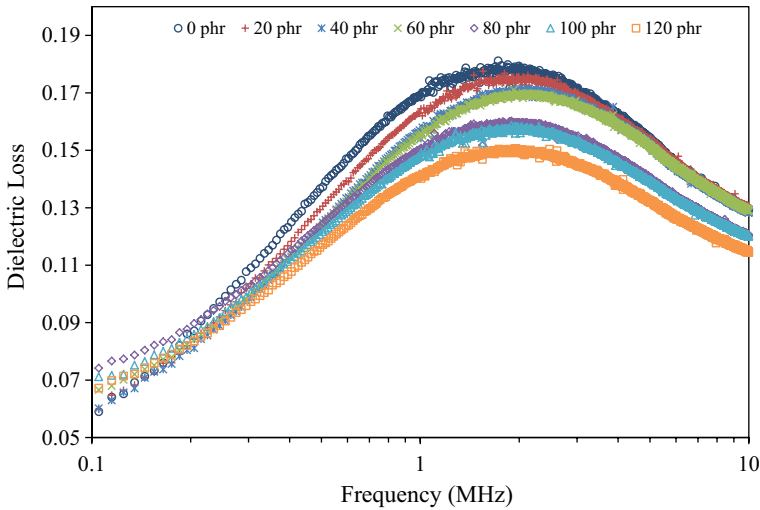
Fig. 12 Electrical properties of different filler content of CCTO embedded in ENR-25 at different frequency ranges of dielectric loss
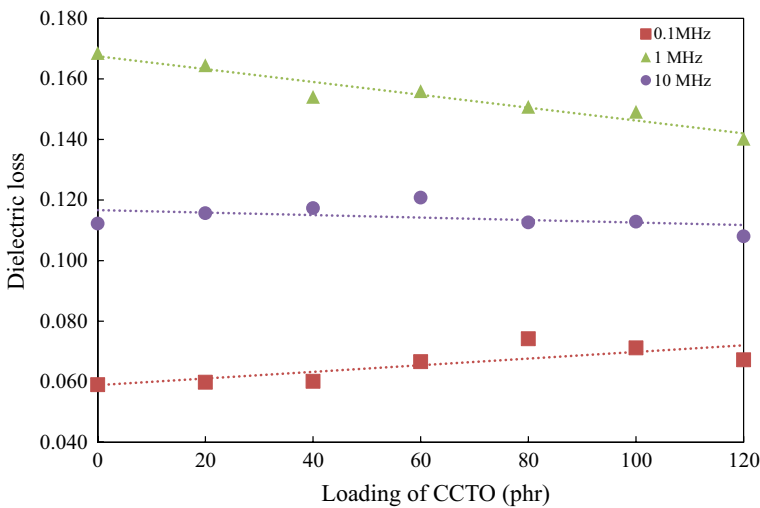

Fig. 13 Dielectric loss curve of different filler content of CCTO embedded in ENR-25 at 0.1, 1, and 10 MHz

tensile strength. The highest tensile strength, 16.46 MPa, was obtained from 40 phr of CCTO loading. The incorporation of CCTO particles lowered the tc_{90} at 20 phr compared to 0 phr. Then, it gradually increased with filler loading of 20 to 120 phr. The hardness properties also showed an increase with polynomial tendency from 30.5 to 44.7 Shore A, indicating the increasing rigidity of the composites with increasing filler content. The highest dielectric permittivity ($\varepsilon_r = 12.114$ at 75 kHz)

and the lowest dielectric loss (tan $\delta = 0.063$ at 75 kHz) were recorded at 120 phr CCTO addition. Therefore, it can be concluded that the optimum properties were obtained from 40 phr filler loading of CCTO/ENR-25. The current study also found that various essential properties of ENR-25 can be successfully modified through the addition of CCTO particles, allowing it to be tailored towards specific applications.

References

1. Ruan M, Yang D, Guo W et al (2018) Improved dielectric properties, mechanical properties, and thermal conductivity properties of polymer composites via controlling interfacial compatibility with bio-inspired method. Appl Surf Sci 439:186–195. https://doi.org/10.1016/j.apsusc.2017.12.250

2. Yang D, Kong X, Ni Y et al (2019) Novel nitrile-butadiene rubber composites with enhanced thermal conductivity and high dielectric constant. Compos Part A Appl Sci Manuf 124:105447. https://doi.org/10.1016/j.compositesa.2019.05.015

3. Yang D, Huang S, Wu Y et al (2015) Enhanced actuated strain of titanium dioxide/nitrile-butadiene rubber composite by the biomimetic method. RSC Adv 5:65385–65394. https://doi.org/10.1039/c5ra12311a

4. Salaeh S, Muensit N, Bomlai P, Nakason C (2011) Ceramic/natural rubber composites: Influence types of rubber and ceramic materials on curing, mechanical, morphological, and dielectric properties. J Mater Sci 46:1723–1731. https://doi.org/10.1007/s10853-010-4990-6

5. Jiang S, Jin L, Hou H, Zhang L (2019) Polymer-based nanocomposites with high dielectric permittivity. Elsevier Inc, Hoboken

6. Sain PK, Goyal RK, Bhargava AK, Prasad YVSS (2014) Thermal and dielectric behavior of flexible polycarbonate/lead zirconate titanate composite system. J Appl Polym Sci 131:1–7. https://doi.org/10.1002/app.39913

7. Subramanian MA, Li D, Duan N et al (2000) High dielectric constant in $ACu_3Ti_4O_{12}$ and $ACu_3Ti_3FeO_{12}$ phases. J Solid State Chem 151:323–325. https://doi.org/10.1006/jssc.2000.8703

8. Sulaiman MA, Hutagalung SD, Mohamed JJ et al (2011) High frequency response to the impedance complex properties of Nb-doped $CaCu_3Ti_4O_{12}$ electroceramics. J Alloys Compd 509:5701–5707. https://doi.org/10.1016/j.jallcom.2011.02.145

9. Li Y, Li W, Du G, Chen N (2017) Low temperature preparation of $CaCu_3Ti_4O_{12}$ ceramics with high permittivity and low dielectric loss. Ceram Int 43:9178–9183. https://doi.org/10.1016/j.ceramint.2017.04.069

10. Li R, Zhou J, Liu H, Pei J (2017) Effect of polymer matrix on the structure and electric properties of piezoelectric lead zirconatetitanate/polymer composites. Mater (Basel) 10:945. https://doi.org/10.3390/ma10080945

11. González N, Custal M, dels À, Tomara GN, et al (2017) Dielectric response of vulcanised natural rubber containing $BaTiO_3$ filler: the role of particle functionalisation. Eur Polym J 97:57–67. https://doi.org/10.1016/j.eurpolymj.2017.10.001

12. Faibunchan P, Nakaramontri Y, Chueangchayaphan W et al (2018) Novel biodegradable thermoplastic elastomer based on poly(butylene succinate) and epoxidized natural rubber simple blends. J Polym Environ 26:2867–2880. https://doi.org/10.1007/s10924-017-1173-4

13. Khumpaitool B, Utara S, Jantachum P (2018) Thermal and mechanical properties of an epoxidised natural rubber composite containing a Li/Cr co-doped NiO-based filler. J Met Mater Miner. https://doi.org/10.14456/jmmm.2018.12

14. Gelling IR (1985) Modification of natural rubber latex with peracetic acid. Rubber Chem Technol 58:86–96

15. Hayeemasae N, Waesateh K, Saiwari S et al (2020) Detailed investigation of the reinforcing effect of halloysite nanotubes-filled epoxidised natural rubber. Polym Bull. https://doi.org/10.1007/s00289-020-03461-4

16. Zaman RA, Abu MJ, Ab Karim S et al (2016) Synthesise CCTO using different mixing media. Mater Sci Forum 840:87–90. https://doi.org/10.4028/www.scientific.net/MSF.840.87

17. Chuayjuljit S, Nutchapong T, Saravari O (2015) Preparation and characterisation of epoxidised natural rubber and epoxidized natural rubber / carboxylated styrene butadiene rubber blends. J Met Mater Miner 25:27–36. https://doi.org/10.14456/jmmm.2015.4

18. Krainoi A, Kummerlöwe C, Nakaramontri Y et al (2018) Influence of critical carbon nanotube loading on mechanical and electrical properties of epoxidised natural rubber nanocomposites. Polym Test 66:122–136. https://doi.org/10.1016/j.polymertesting.2018.01.003

19. Saidina DS, Mariatti M, Julie MJ (2014) Properties of calcium copper titanate and barium titanate filled epoxy composites for electronic applications: effect of filler loading and hybrid fillers. J Mater Sci Mater Electron 25:4923–4932. https://doi.org/10.1007/s10854-014-2253-z

20. Muhamad Sharifuddin S, Mat Nor MS, Mohd Pabli FA et al (2020) Thermal and dynamic mechanical behaviours of CCTO/ENR-25 composite. Mater Sci Forum 1010:274–279. https://doi.org/10.4028/www.scientific.net/msf.1010.274

21. Dahham OS, Noriman NZ, Sam ST et al (2016) The effects of trans-polyoctylene rubber (TOR) as a compatibilizer on the properties of epoxidised natural rubber/recycled silicone catheter (ENR-25/rSC) vulcanizate. MATEC Web Conf. https://doi.org/10.1051/matecconf/20167801076

22. Ondrušová D, Labaj I, Pajtášová M, Vršková J (2019) Preparation and properties of new elastomeric systems containing alternative fillers. MATEC Web Conf 254:07003. https://doi.org/10.1051/matecconf/201925407003

23. Luangchuang P, Chueangchayaphan N, Sulaiman MA, Chueangchayaphan W (2021) High permittivity ceramics-filled acrylonitrile butadiene rubber composites: influence of acrylonitrile content and ceramic type. Polym Bull 78:1755–1769. https://doi.org/10.1007/s00289-020-03181-9

24. Mohamad Z, Ismail H, Thevy RC (2006) Characterisation of epoxidised natural rubber/ethylene vinyl acetate (ENR-50/EVA) blend: Effect of blend ratio. J Appl Polym Sci 99:1504–1515. https://doi.org/10.1002/app.22154

25. Intharapat P, Kongnoo A, Kateungngan K (2013) The potential of chicken eggshell waste as a bio-filler filled epoxidized natural rubber (ENR) composite and its properties. J Polym Environ 21:245–258. https://doi.org/10.1007/s10924-012-0475-9

26. Dang Z-M, Yuan J-K, Zha J-W et al (2012) Fundamentals, processes and applications of high-permittivity polymer–matrix composites. Prog Mater Sci 57:660–723. https://doi.org/10.1016/j.pmatsci.2011.08.001

27. Mrudula MS, Gopinathan Nair MR (2020) Dielectric properties of natural rubber/polyethylene oxide block copolymer complexed with transition metal ions. Polym Bull 77:6029–6048. https://doi.org/10.1007/s00289-019-03035-z

28. Kato A, Kokubo Y, Tsushi R, Ikeda Y (2014) Hydrophobic and hydrophilic silica-filled cross-linked natural rubber (NR): structure and properties chemistry manufacture and applications of natural rubber. Elsevier Inc, Hoboken, pp 193–215

29. Rattanasom N, Poonsuk A, Makmoon T (2005) Effect of curing system on the mechanical properties and heat aging resistance of natural rubber/tire tread reclaimed rubber blends. Polym Test 24:728–732. https://doi.org/10.1016/j.polymertesting.2005.04.008

30. Arguello JM, Santos A (2016) Hardness and compression resistance of natural rubber and synthetic rubber mixtures. J Phys Conf Ser 687:012088. https://doi.org/10.1088/1742-6596/687/1/012088

31. Ramajo LA, Ramírez MA, Bueno PR et al (2008) Dielectric behaviour of CaCu3Ti4O12 -epoxy composites. Mater Res 11:85–88. https://doi.org/10.1590/S1516-14392008000100016

32. Larguech S, Triki A, Ramachandran M, Kallel A (2020) Dielectric properties of jute fibers reinforced poly(lactic acid)/poly(butylene succinate) blend matrix. J Polym Environ. https://doi.org/10.1007/s10924-020-01927-0

Authors and Affiliations

Syifa' Muhammad Sharifuddin[1] · Mohd Shukri Mat Nor[1] · Fathin Asila Mohd Pabli[1] · Wannarat Chueangchayaphan[2] · Zainal Arifin Ahmad[3] · Muhammad Azwadi Sulaiman[1]

✉ Muhammad Azwadi Sulaiman
   azwadi@umk.edu.my

[1]   Advanced Materials Research Cluster, Faculty of Bioengineering and Technology, Universiti Malaysia Kelantan, 17600 Jeli, Kelantan, Malaysia

[2]   Faculty of Science and Industrial Technology, Prince Songkla University, Surat Thani Campus, Surat Thani 84000, Thailand

[3]   School of Materials and Mineral Resources Engineering, Universiti Sains Malaysia, 14300 Nibong Tebal, Penang, Malaysia